Analytical Prediction of Store Separation Characteristics from Subsonic Aircraft

Marnix F. E. Dillenius,* Frederick K. Goodwin,* and Jack N. Nielsen†
Nielsen Engineering & Research, Inc., Mountain View, Calif.

This paper presents a predictive method valid up to the critical speed for determining the six degree-of-freedom trajectories of stores released from single, TER, or MER configurations mounted on realistic aircraft. A computer program has been developed to calculate the aerodynamic forces and the trajectory. The paper also presents comparisons with data selected from an extensive wind-tunnel test program designed to test the theory through systematic measurements. Generally, the method predicts accurately the experimentally measured flowfields, store loadings, and six-degree-of-freedom trajectories.

Nomenclature

C_m = store pitching-moment coefficient, pitching moment/$q_\infty S_r \ell_r$; see Fig. 3
C_n = store yawing-moment coefficient, yawing moment/$q_\infty S_r \ell_r$; see Fig. 3
C_N = store normal-force coefficient, normal force/$q_\infty S_r$; see Fig. 3
C_Y = store side-force coefficient, side force/$q_\infty S_r$; see Fig. 3
C_l = store rolling-moment coefficient, rolling moment/$q_\infty S_r \ell_r$; see Fig. 3
d = maximum store diameter
ℓ_r = reference length, taken equal to d
ℓ_s = store length
M_∞ = freestream Mach number
q_∞ = freestream dynamic pressure
s = wing semispan
S_r = reference area, $\pi d^2/4$
t = time, sec
U_s, V_s, W_s = components of local flow velocity in store coordinate system; see Fig. 3
V_∞ = freestream velocity
V_{∞_s} = freestream velocity as seen by the store
W_B = local flow velocity in the upwards direction measured under the fuselage
x_B, y_B, z_B = fuselage coordinate system with origin at the nose tip, x positive upstream from the nose tip, y positive to the right, and z positive down
x_s, y_s, z_s = store coordinate system; see Fig. 3
y = lateral location measured from fuselage longitudinal axis, positive to right facing forward
α = airplane and store angle of attack
Δz = distance of store beneath its attached position, positive downward
$\Delta\Psi, \Delta\Theta, \Delta\Phi$ = changes in yaw, pitch, and roll angles, respectively, of store from time $=0$ values; positive nose to the right, nose up, and right wing down, respectively
ξ, η, ζ = axial, lateral, and vertical displacements, respectively, of the store center of gravity relative to the carriage position on the pylon or TER in the fuselage coordinate system; positive forward, to the right, and downward, respectively.
ϕ = roll attitude of store; $\phi=0$ for empennage panel in vertical location

Presented as Paper 74-775 at the AIAA Mechanics and Control of Flight Conference, Anaheim, California, August 5-9, 1974; submitted September 13, 1974; revision received January 20, 1975. This work was supported by the Air Force Flight Dynamics Laboratory, Air Force Systems Command, Wright-Patterson Air Force Base, Ohio, under Contracts F33615-69-C-1337, F33615-71-C-1116, and F33615-72-C-1375.

Index categories: Aircraft Aerodynamics (including Component Aerodynamics); LV/M Trajectories.

*Research Engineer. Member AIAA.
†President. Fellow AIAA.

Introduction

An analytical method for accurately predicting external store separation characteristics saves time and money in preliminary design and wind-tunnel testing of the store and parent aircraft. To provide such a tool, a combined theoretical/experimental investigation was undertaken with the goal of producing a rational scheme capable of predicting the forces and moments acting on external stores and their trajectories when released from a parent aircraft.

In the early stages of the work, methods were developed to predict three-degree-of-freedom store separation characteristics from simplified swept-wing aircraft with circular fuselages.[1] Gradually, the theory was extended to six degrees of freedom and some of the configuration restrictions were relaxed.[2] In the latest work, the circular fuselage restriction was removed and engine air inlets were also modeled.[3,4]

Simultaneously with the analytical work, an extensive experimental program was carried out to test the theory and isolate important effects through systematic measurements of flowfields, store load distributions, store forces and moments, and captive-store trajectories. These data[5-9] were taken in the 4-T Tunnel at the Arnold Engineering Development Center (AEDC). The basic wind-tunnel model was an uncambered fuselage with circular cross section. Through the systematic addition of a wing, pylon, ejection rack, noncircular fuselage attachment, engine inlets with variable blockage to the flow, canopy and cambered nose, important interference effects could be isolated.

The first objective of this paper is to summarize the predictive method valid up to the critical speed for analytically determining: 1) flowfield induced by a parent aircraft; 2) load distributions and forces and moments on a store with or without empennage in a nonuniform flowfield; and 3) six-degree-of-freedom trajectory characteristics of a store released from the parent aircraft. The second objective is to present comparisons with data obtained during the wind-tunnel test program. Comparisons are presented between measured flowfields, store load distributions, forces and moments, captive-store trajectories, and those predicted by the theory.

The predictive method is unique in that specification of aerodynamic coefficients is not required except for an axial drag coefficient for the released store. The computer program determines the other coefficients. The program only requires knowledge of the geometry of the parent aircraft and stores and the flight conditions of the parent aircraft. The computer program has been used as the data-generating part of an interactive graphic application capable of visually displaying predicted store separation trajectories.[4] This work was performed by C. L. Dyer at AFFDL. A permanent visual documentation system recently set up by Spahr[10] at Sandia Labs. in connection with the study of aircraft delivered weapons also employs the computer program.

Summary of Analytical Method

The method applies to a fighter-bomber-type aircraft which can be made up of a fuselage, wing, pylon, rack, and stores. Consider a store in the immediate vicinity of the airframe. The store is first considered in uniform flow and its volume effect on the wing-pylon loading is computed. The nonuniform flowfield produced by the airframe is then determined. The store loading is calculated from this nonuniform flowfield in which the store is immersed. As a second iteration, the store could be placed in this nonuniform flowfield and the wing loading recalculated. The additional effect on the store caused by the refined wing loading has been shown to be small.[1] The calculation is therefore stopped after the first iteration. In this way, most of the mutual interference between aircraft and store is accounted for without the need to solve the complete interference problem at each point in the trajectory. This has the effect of significantly reducing computer time. To calculate the nonuniform flowfield, the various components of the airframe are mathematically modeled as will be described. An application of the Prandtl-Glauert rule accounts for compressibility effects.

Wing-Pylon

A vortex-lattice method[3] is used to account for basic wing effects of angle of attack, dihedral, twist, and camber. Finite length source panels, which are narrow in the streamwise direction, represent the wing thickness effect. The pylon is represented in a similar manner and full mutual interference between wing and pylon is accounted for. The elementary vortex strengths associated with the vortex lattice determine the wing-pylon loading. Their magnitudes are obtained from the solution to a set of simultaneous equations that result from applying the flow tangency conditions at control points.

Circular Fuselage, Stores, and Ejector Racks

These bodies of revolution are modeled by a distribution of three-dimensional point sources and sinks along the longitudinal axis of the body to account for volume effects.[1] In the case of the fuselage, two-dimensional doublets placed on the axis account for angle of incidence.[3] The source and sink strengths are determined from a set of simultaneous equations that result from applying the flow tangency condition at points on the surface of the body of revolution.

Noncircular Fuselage and Air Inlets

The method employed to model fuselages with noncircular cross sections[3] is based on the equivalence rule which states that far away from a general slender body the flow becomes axisymmetric and equal to the flow around the equivalent body of revolution. A solution valid for the entire flowfield is given by a composite solution consisting of 1) a three-dimensional potential associated with the equivalent body of revolution, 2) a two-dimensional sink term, and 3) an inner crossflow solution made up of polar harmonics and a two-dimensional source term. At large distances, the higher-order polar harmonics die out, the two-dimensional source term cancels the sink term and the flow is axisymmetric. Air inlet effects are also treated in this manner. The streamwise body slopes which are calculated on the basis of the inlets being closed are modified to reflect the air inlet velocity ratio.

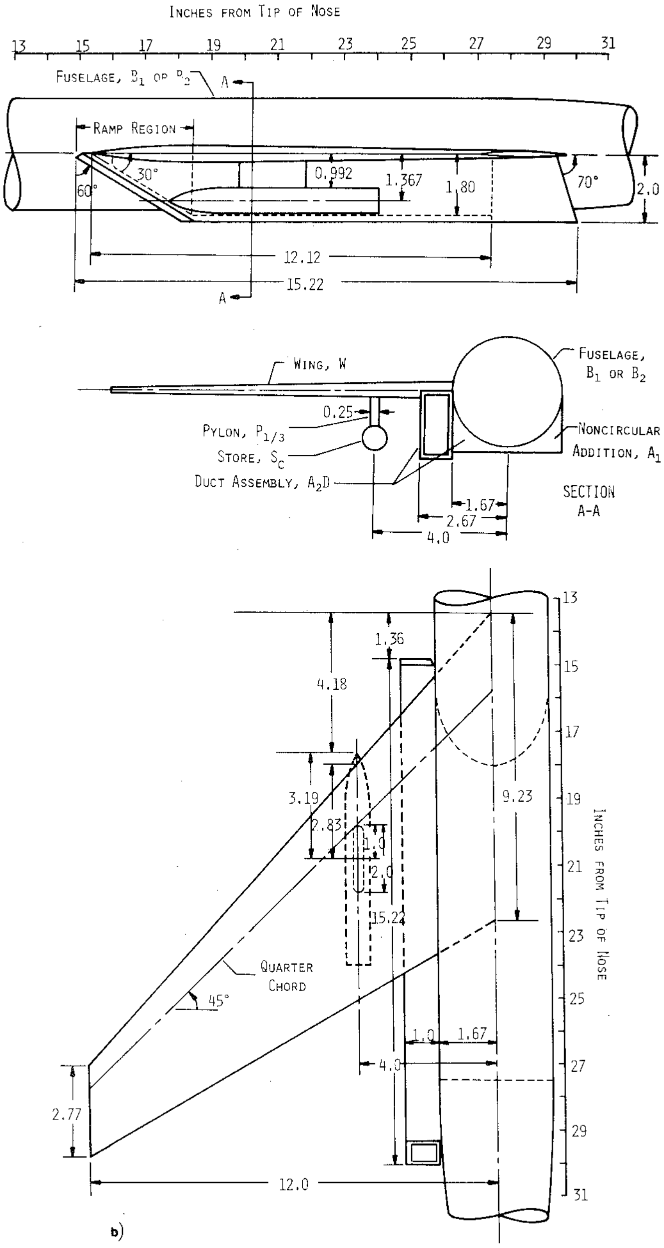

Fig. 1 Wind-tunnel model a) Wing and duct attached to circular fuselage. b) Top view of wing and duct attached to circular fuselage.

Wing-Fuselage Interference

Wing-fuselage interference effects are accounted for by first including the effects of the fuselage on the vortex lattice laid out on the exposed wing panels and then imaging the lattice inside the fuselage.[3]

Calculation of Store Forces, Moments and Trajectories

The methods for calculating the forces and moments[2] due to the store body and planar or cruciform empennage immersed in a nonuniform stream are based on slender-body theory. Reverse flow theorems with aspect ratio correction are used for the empennage. Panel-panel interference effects are included. The trajectory method[2] utilizes the full six-degree-of-freedom equations. It is not required that the principal axes of inertia coincide with the axes of symmetry of the store. At each step in the trajectory calculation, the nonuniform flowfield in the vicinity of the store and the resulting forces and moments acting on the store are determined.

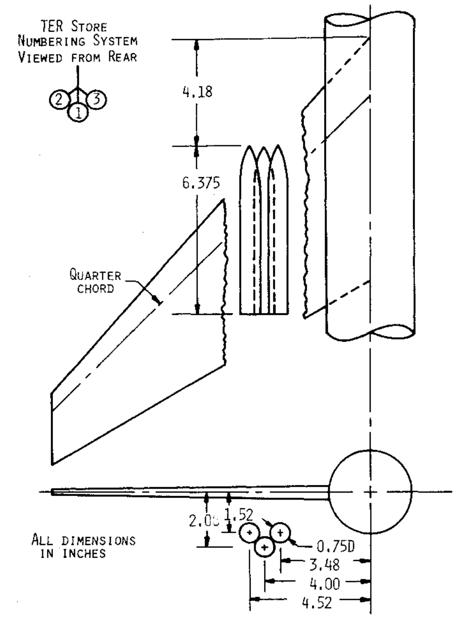

Fig. 2 TER arrangement under the wing; pylon and TER not shown.

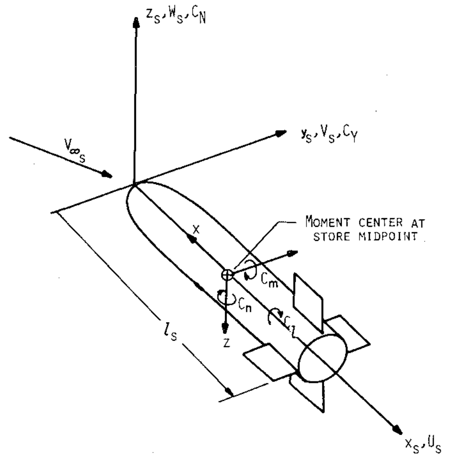

Fig. 3 Store coordinate system and positive velocity and force and moment directions.

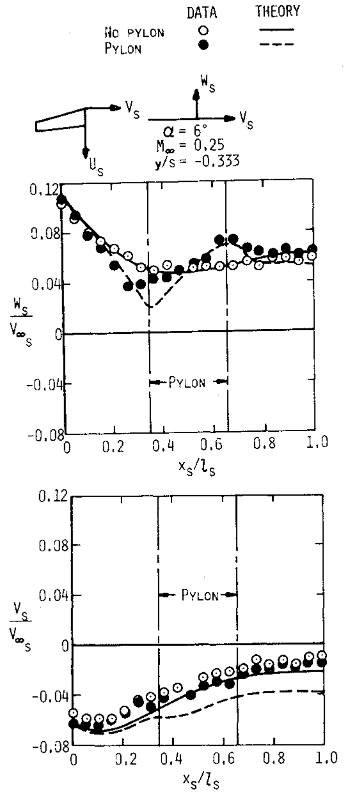

Fig. 4 Effect of pylon on flowfield of wing-circular fuselage combination.

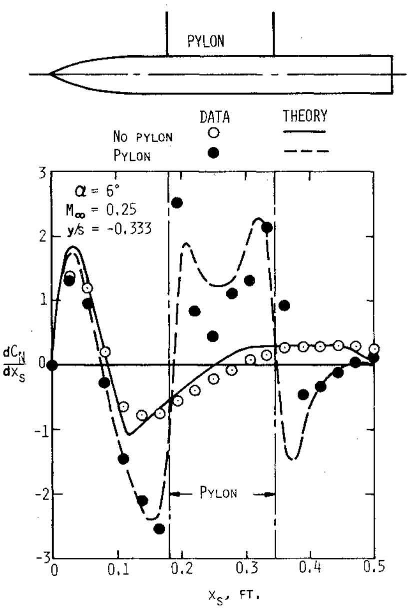

Fig. 5 Effect of pylon on normal-force distribution of attached store.

Comparisons Between Measurements and Predictions

The experimental data discussed in this paper were obtained using the following wind-tunnel model configurations: 1) the wing with circular fuselage (B_1 or B_2 in Fig. 1), pylon, and store at the one-third semispan location; 2) the wing with circular fuselage combination of Fig. 1 with the pylon, TER rack, and three stores at the one-third semispan location; Fig. 2; 3) wing and either the noncircular addition A_1 or duct assembly A_2D attached to the circular fuselage; Fig. 1. In some cases the pylon was present.

The ogive-cylinder store was tested singly with and without empennage and in the TER configuration without empennage. A pressure-instrumented version without empennage was used to obtain load distributions. The store coordinate system and positive velocity and force and moment directions are shown in Fig. 3.

Effects of Pylon on Flowfield and Attached Store Load Distribution

Sidewash and upwash velocities are shown in Fig. 4 for 6° angle of attack and Mach number 0.25 at the position the centerline of the attached store would occupy if it were present at the one-third semispan position of the left wing panel. Data with and without the pylon present are compared with theory. The sidewash is outboard everywhere, and there is a small measured effect of the pylon on the sidewash which is less than the predicted effect. There is a large upwash along the store centerline, and its modification due to the pylon is well predicted by the theory. The normal-force distribution along the finless store caused by the upwash field just described is shown in Fig. 5. It is seen that the load distribution with the pylon present is very irregular and is predicted quite well.

Flowfields and Loading Prediction for TER Configurations

In this section the comparisons to be presented are for the TER grouping shown in Fig. 2. The TER and the pylon are not shown in Fig. 2 for clarity. The stores are at the one-third semispan location and the Mach number is 0.25.

The flowfield has been measured for a number of positions beneath the TER configuration with the bottom store missing. The TER rack is longer than the pylon and has been approximated by a body of revolution in the prediction method.

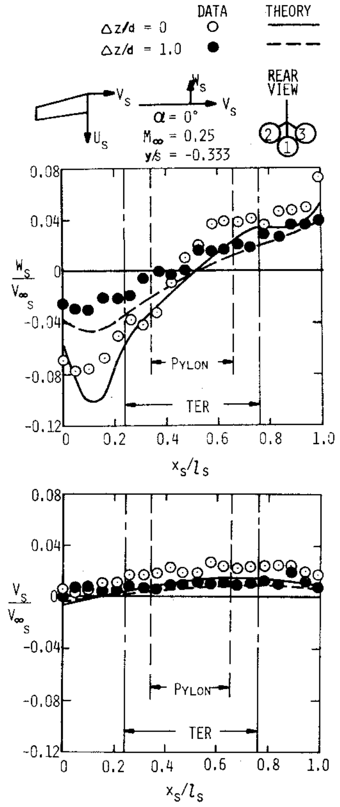

Fig. 6 Effect of vertical position on flowfield under TER configuration.

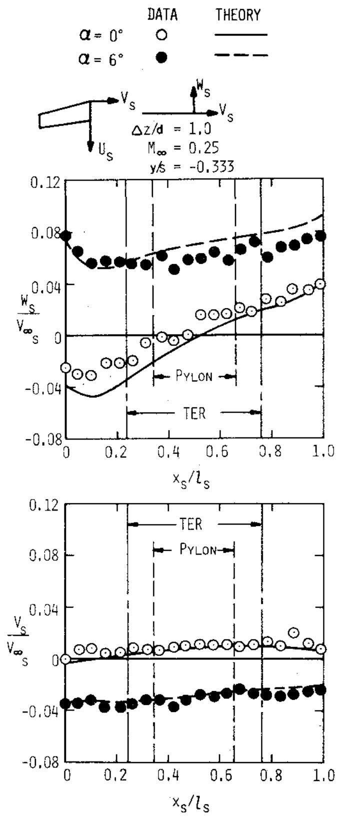

Fig. 7 Effect of angle of attack on flowfield under TER configuration.

The sidewash and upwash are shown in Fig. 6 along the position the axis of store S_1 would occupy for the attached store location, $\Delta z/d = 0$, and for one diameter below the attached locations $\Delta z/d = 1.0$. There is considerable difference in the upwash between these vertical locations which is well predicted by the theory. In the theory the effect of the shoulder stores S_2 and S_3 has been predicted using three-dimensional source terms.

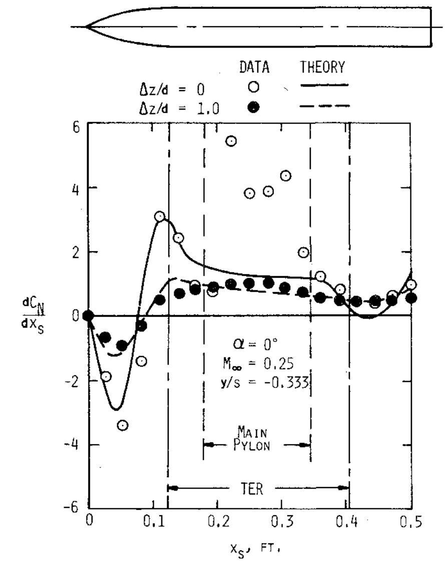

Fig. 8 Effect of vertical position on normal-force distribution of store S_1.

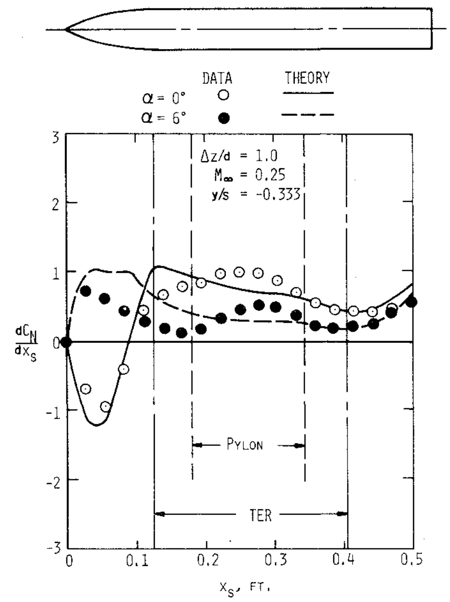

Fig. 9 Effect of angle of attack on normal-force distribution of store S_1.

The variations of sidewash and upwash with angle of attack are shown in Fig. 7 for $\Delta z/d = 1.0$. Both are predicted well for $\alpha = 0°$ and $\alpha = 6°$. The calculative method thus predicts well the effects of vertical location and angle of attack of the aircraft on the flowfield acting on the store S_1. The normal-force distributions on store S_1 for the attached store and for a location one diameter below the attached position are shown in Fig. 8. The loading on the attached store is somewhat underpredicted in the region spanned by the main pylon. This is caused by not accounting for the short pylon which is part of the rack. However, one diameter beneath the pylon the prediction is very good. The effect of angle of attack on the normal-force distribution on S_1 is shown in Fig. 9 for $\Delta z/d = 1.0$. Experiment and theory are in good agreement for both angles of attack.

Effects of Empennage on Store Forces

Comparison between experiment and theory for forces caused by the presence of the empennage are now presented. In order to test the method of determining the empennage forces without introducing errors from the theoretically obtained nonuniform flowfield, experimental flowfield data have been used in the calculations.

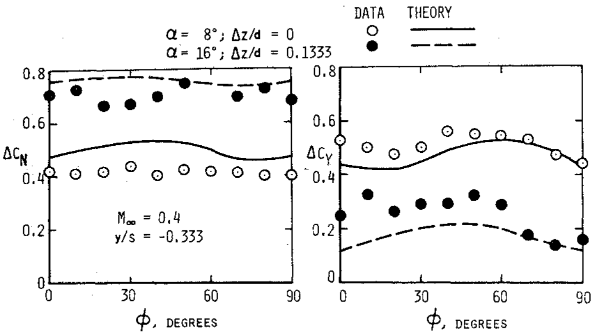

Fig. 10 Empennage contributions to normal-force and side-force coefficients.

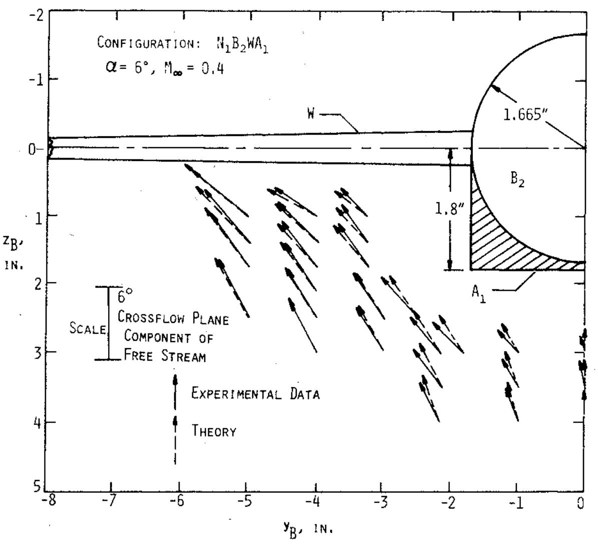

Fig. 11 Velocity vector plot for crossflow plane 19.66 in. aft of nose tip.

In Fig. 10, the forces for the finned store mounted at or near the attached positon (see Fig. 1) are shown as a function of roll angle and compared with theory for angles of attack of 8° and 16°. A roll angle of 0° places the fins vertical and horizontal. The incremental coefficients are the difference between the coefficients with the empennage on and with the empennage off. The theory is in fair agreement with the data at both angles of attack.

Effects of Noncircular Fuselage and Inlets on Flowfields

Figure 11 shows a crossflow plane velocity vector plot for the noncircular fuselage model with the wing attached. The angle of attack is 6°. The results predicted by the theory agree well with the experimental data thereby illustrating the validity of the wing-fuselage interference method. The axial location is aft of the ramp region of the noncircular addition (see Fig. 1).

Distributions of upwash under the fuselage centerline for the various stages of the wind-tunnel model build-up and various inlet velocity ratios are plotted in Fig. 12. The angle of attack is 0°. Figure 12a shows the effect of model build-up. The three models are circular body with wing N_1B_2W, circular body with wing and noncircular addition $N_1B_2WA_1$, and circular body with wing and duct assembly $N_1B_2WA_2D$. For the latter configuration, the ratio of inlet or duct velocity to the freestream velocity, V_D/V_∞, is 1.0. The effects of adding the noncircular addition and duct assembly are seen to be most pronounced near the end of the ramp region. In general, the trends are indicated by the theory. The magnitudes of the changes in upwash are predicted only in part.

Figure 12b shows the effect of inlet velocity ratio on the upwash distribution. The effect of reducing the inlet velocity ratio is to increase the downwash very strongly near the end of the ramp region. The theory predicts this effect partially. Just downstream of the ramp region slight flow separation may have occurred. The effect would be to increase the downwash. This separation effect is Reynolds number dependent and would be reduced with higher Reynolds number.

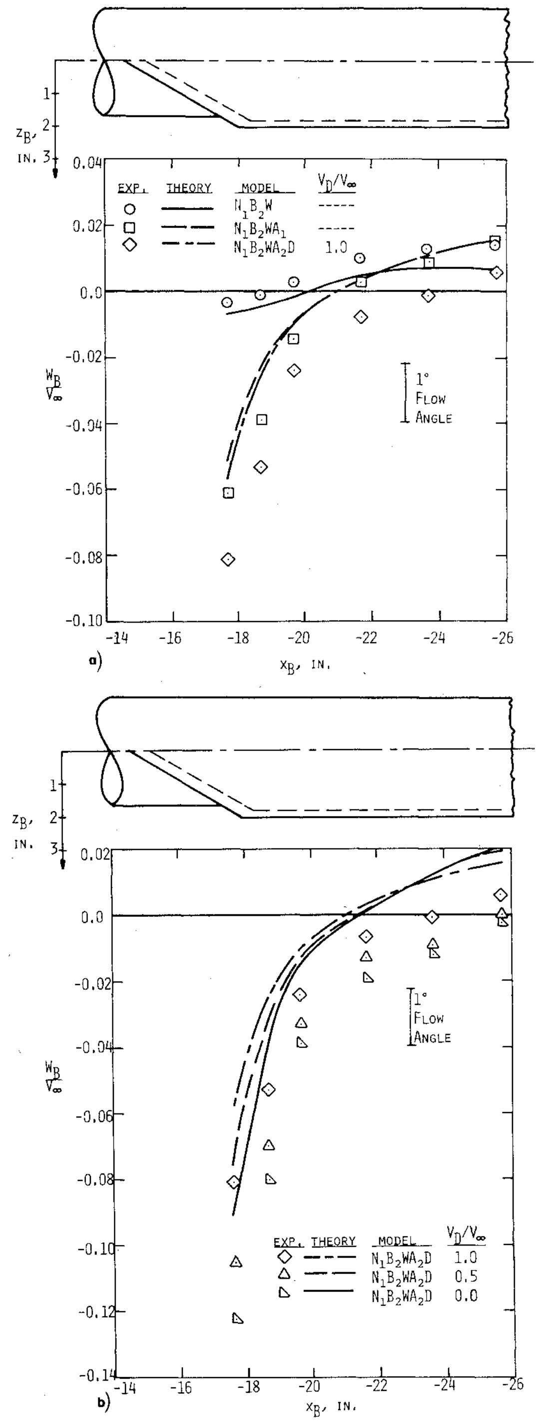

Fig. 12 Distribution of upwash 3 in. under the fuselage centerline; $\alpha = 0°$, $M_\infty = 0.4$; a) Effects of wind-tunnel model build-up. b) Effects of inlet velocity ratio.

All wind-tunnel data presented in this section were obtained at a Reynolds number of 3.4×10^6/ft and a Mach number of 0.4. Actual flight conditions would result in an order of magnitude higher Reynolds numbers. The accuracy of the flow prediction methods described here should increase when applied at flight Reynolds numbers.

Effects of Noncircular Fuselage and Air Inlets on Store Loadings

The normal-force distribution along the finless store, in the position shown in Fig. 1 but with the pylon removed, is

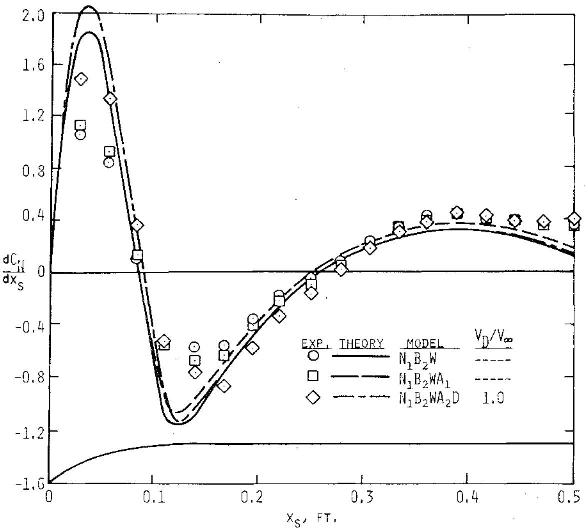

Fig. 13 Effect of wind-tunnel model build-up on the normal-force distribution; $\alpha = 6°$, $M_\infty = 0.4$.

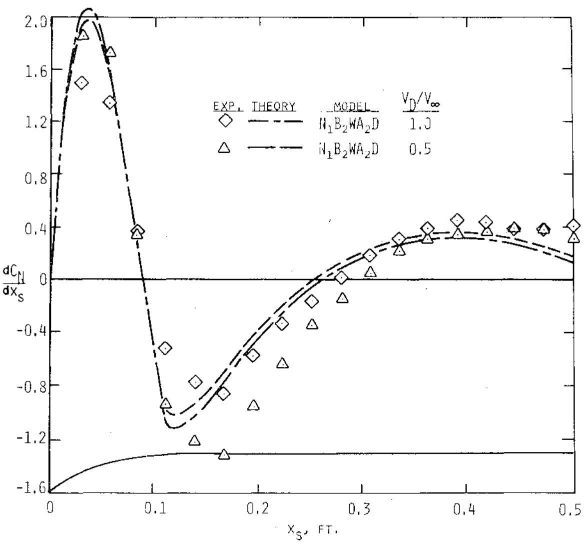

Fig. 14 Effect of inlet velocity ratio on the normal-force distribution; $\alpha = 6°$, $M_\infty = 0.4$.

illustrated in Fig. 13 for the various stages of the model build-up. The half-store silhouette is outlined along the horizontal axis. The angle of attack is 6°. The normal-force distribution is affected very little by the fuselage build-up. Agreement between theory and experiment in loading is good.

Figure 14 shows the effect of inlet velocity ratio on the loading distribution. When the ratio is reduced to one half, the measured local normal force is reduced in the region just aft of the store nose. This is not predicted by the theory. The discrepancy can be explained by the presence of a vortex near the lower outside corner of the inlet. The effect of this vortex would be reduced with higher Reynolds number.

Trajectory Studies

The methods of flowfield predictions and store force and moment determinations have been combined into one program with the six-degree-of-freedom equations of motion to yield a trajectory prediction method. A number of sample trajectories have been run to provide predictions for comparison with experimental captive-store trajectories.

In order to represent full-scale conditions, the wind-tunnel models have been scaled up by a factor of twenty. Initial store and aircraft angles of attack are equal. For the two cases considered below, the parent aircraft configuration consists of the wing with the circular fuselage. The pylon is attached to the left wing panel.

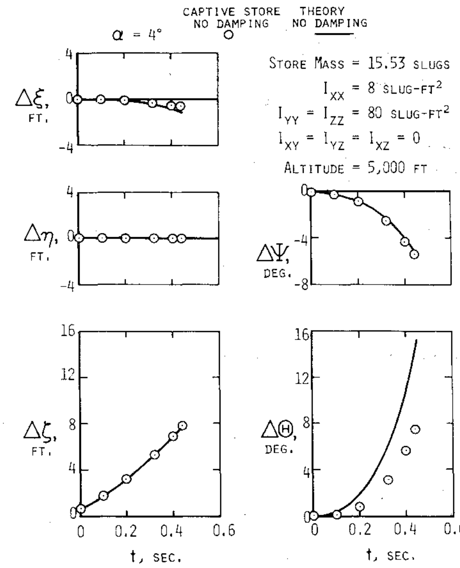

Fig. 15 Comparison between calculated trajectory and captive-store trajectory of finless store; $M_\infty = 0.4$.

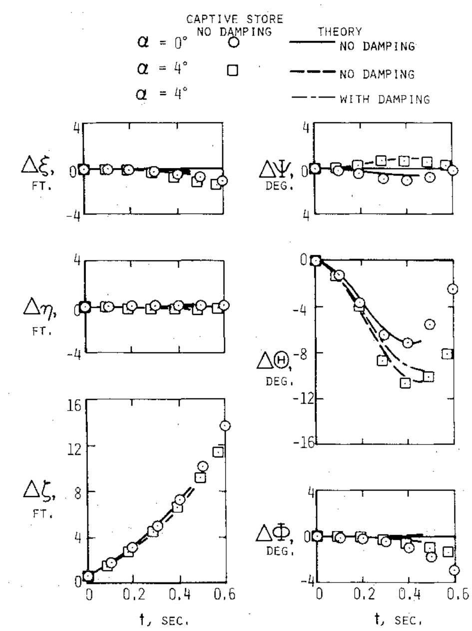

Fig. 16 Comparison between calculated trajectories and captive-store trajectories of store with empennage; $M_\infty = 0.4$.

A comparison between the calculated trajectory and the captive-store trajectory for the case of no aerodynamic damping is shown in Fig. 15 for the store with no empennage. It is released at time $t = 0$ one store radius beneath its attached position on the pylon with an initial downward velocity of 10 fps. For both the aircraft and the store, $\alpha = 4°$. In Fig. 15, the three left-hand curves show the position of the store center of gravity relative to its attached position. The left-hand curves show a slight rearward movement of the store, no lateral movement, and a vertical movement equivalent to free fall. The two right-hand curves show a substantial yaw of the store nose outboard and a large pitch up of the store which is somewhat overpredicted by the computer program.

A comparison similar to that of Fig. 15 is shown in Fig. 16 for the same store and initial conditions except that the cruciform empennage has been added to produce static stability. Results are shown for angles of attack of $\alpha = 0°$ and $\alpha = 4°$. The store center of mass coordinates show the same general behavior as the previous case. The pitching and yawing motions from the computer program and the captive-store trajectory are in good agreement for both angles of attack.

To assess the importance of damping on the motion, the trajectory was also calculated including damping in all three angular motions. The damping effect is negligible except in the pitching oscillation which was reduced in maximum amplitude by about one degree.

Conclusions

A rational method for calculating six-degree-of-freedom trajectories of external stores released from modern aircraft valid up to the critical speed has been presented. The method involves flowfield predictions, store force and moment predictions, and trajectory calculations. Generally good agreement between experiment and prediction is shown in detailed comparisons. In all phases of the development of the method, the simplest flow models consistent with the desired accuracy have been used. This has resulted in minimizing the computer time required to calculate a trajectory. Thus, the program should save time and money in preliminary design and should provide a tool for minimizing costly wind-tunnel testing. A typical trajectory calculation on the Control Data Corp. 6600 takes 3-5 min.

References

[1] Goodwin, F. K., Nielsen, J. N., and Dillenius, M. F. E., "Method for Predicting Three-Degree-of-Freedom Store Separation Trajectories at Speeds up to the Critical Speed," AFFDL-TR-71-81, Nov. 1974, Air Force Flight Dynamics Lab., Wright-Patterson Air Force Base, Ohio.

[2] Goodwin, F. K., Dillenius, M. F. E., and Nielsen, J. N., "Prediction of Six-Degree-of-Freedom Store Separation Trajectories at Speeds Up to the Critical Speed," Vol. I—*Theoretical Methods and Comparisons with Experiment* and Vol. II—*User's Manual for the Computer Programs,* AFFDL-TR-72-83, Oct. 1974, Air Force Flight Dynamics Lab., Wright-Patterson Air force Base, Ohio.

[3] Dillenius, M. F. E., Goodwin, F. K., and Nielsen, J. N., "Extension of the Method for Predicting Six-Degree-of-Freedom Store Separation Trajectories at Speeds up to the Critical Speed to Include a Fuselage with Noncircular Cross Section," Vol. I—*Theoretical Methods and Comparisons with Experiment* and Vol. II—*User's Manual for the Computer Program*, AFFDL-TR-74-130, Nov. 1974, Air force Flight Dynamics Lab., Wright-Patterson Air force Base, Ohio.

[4] Dillenius, M. F. E., Goodwin, F. K., Nielsen, J. N., and Dyer, C. L., "Extensions to the Method for Prediction of Six-Degree-of-Freedom Store Separation Trajectories at Speeds up to the Critical Speed, Including Interactive Graphics Applications and Bodies of Arbitrary Cross Section," *Proceedings of the Symposium on Aircraft/Stores Compatibility,* JTCG/ALNNO WP-12-2, Vol. II, 1973, pp. 135-207.

[5] Summers, W. E., "Flow Field Characteristics and Aerodynamic Loads on External Stores near the Fuselage and Wing Pylon Positions of a Swept-Wing/Fuselage Model at Mach Numbers of 0.25 and 0.70," AEDC-TR-70-202, Sept. 1970, Arnold Engineering Development Center, Tullahoma, Tenn.

[6] Roberts, R. H., "Flow-Field Characteristics and Aerodynamic Loads on External Stores Near the Fuselage and Wing Pylon Positions of a Swept-Wing/Fuselage Model at Mach Numbers of 0.25, 0.40, and 0.70—Phase II," AEDC-TR-70-279, Jan. 1971, Arnold Engineering Development Center, Tullahoma, Tenn.

[7] Roberts, R. H., "Flow-Field Characteristics and Aerodynamic Loads on External Stores near the Fuselage and Wing Pylon Positions of a Swept-Wing/Fuselage Model at Mach Numbers of 0.40 and 0.70—Phase III," AEDC-TR-71-73, April 1971, Arnold Engineering Development Center, Tullahoma, Tenn.

[8] Roberts, R. H., "Flow-Field Characteristics and Aerodynamic Loads on External Stores near the Fuselage and Wing Pylon Positions of a Swept-Wing/Fuselage Model at Mach Numbers of 0.40 and 0.70—Phase IV," AEDC-TR-71-208, Oct. 1971, Arnold Engineering Development Center, Tullahoma, Tenn.

[9] Roberts, R. H. and Meyers, J. R., "Flow-Field Characteristics and Aerodynamic Loads on External Stores near the Fuselage and Wing Pylon Position of a Swept-Wing fuselage Model at Mach Numbers of 0.4 and 0.7—Phase V," AEDC-TR-73-87, March 1974, Arnold Engineering Development Center, Tullahoma, Tenn.

[10] Spahr, H. R., "Computer Generated Visual Documentation of Theoretical Store Separation Analyses," *Proceedings of the Symposium on Aircraft/Stores Compatibility*, JTCG/ALNNO WP-12-2, Vol. II, 1973, pp. 207-237.